iScience

CellPress
OPEN ACCESS

Article

Excitable dynamics of flares and relapses in autoimmune diseases

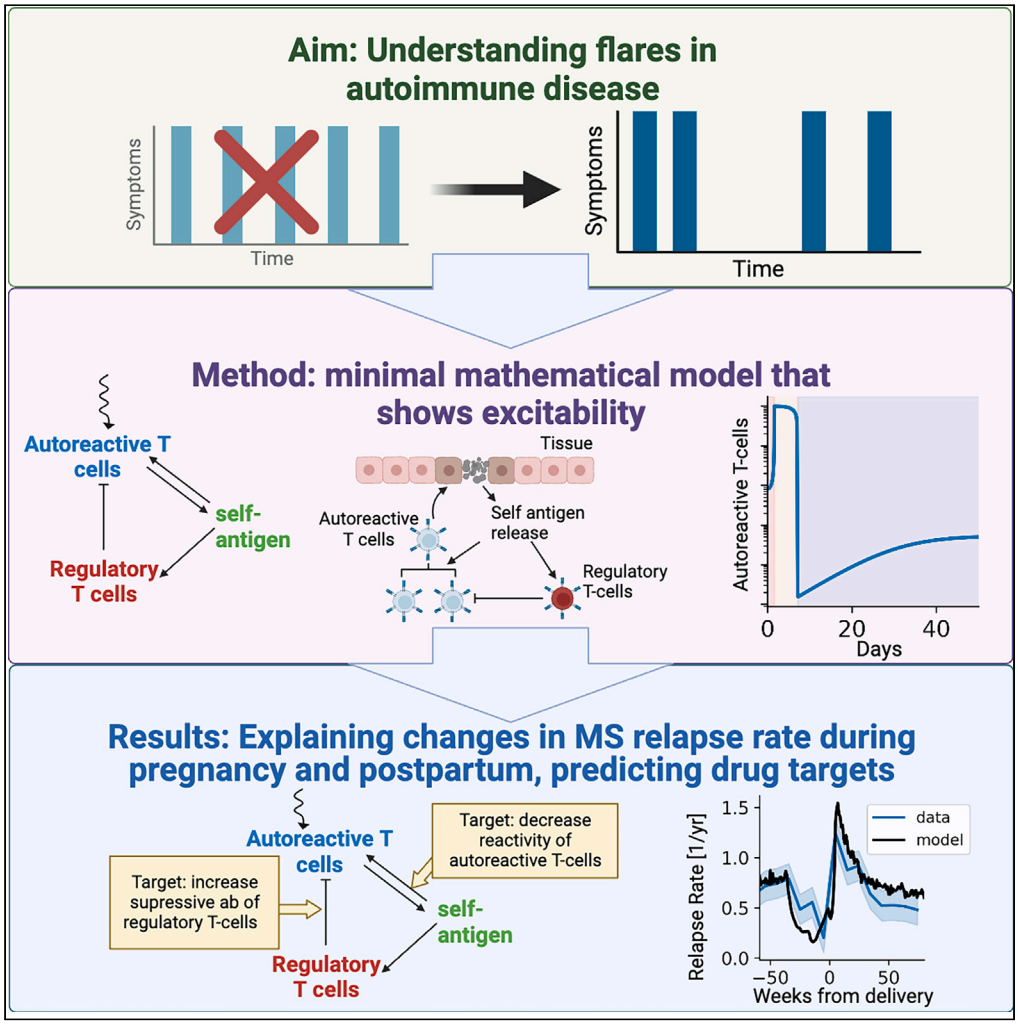

Yael Lebel, Tomer Milo, Alon Bar, Avi Mayo, Uri Alon

uri.alon@weizmann.ac.il

Highlights

Model suggests excitable mechanism for autoimmune flares

Lymphocyte dynamics explain changes in relapse rates during pregnancy and postpartum

Model identifies intervention strategies for autoimmune diseases

Parameter sensitivity reveals how mild changes shape disease progression

Lebel et al., iScience *26*, 108084
November 17, 2023
https://doi.org/10.1016/j.isci.2023.108084

iScience

CellPress
OPEN ACCESS

Article

Excitable dynamics of flares and relapses in autoimmune diseases

Yael Lebel,[1] Tomer Milo,[1] Alon Bar,[1] Avi Mayo,[1] and Uri Alon[1,2,*]

SUMMARY

Many autoimmune disorders exhibit flares in which symptoms erupt and then decline, as exemplified by multiple sclerosis (MS) in its relapsing-remitting form. Existing mathematical models of autoimmune flares often assume regular oscillations, failing to capture the stochastic and non-periodic nature of flare-ups. We suggest that autoimmune flares are driven by excitable dynamics triggered by stochastic events auch as stress, infection and other factors. Our minimal model, involving autoreactive and regulatory T-cells, demonstrates this concept. Autoimmune response initiates antigen-induced expansion through positive feedback, while regulatory cells counter the autoreactive cells through negative feedback. The model explains the decrease in MS relapses during pregnancy and the subsequent surge postpartum, based on lymphocyte dynamics. Additionally, it identifies potential therapeutic targets, predicting significant reduction in relapse rate from mild adjustments of regulatory T cell activity or production. These findings indicate that excitable dynamics may underlie flare-ups across various autoimmune disorders, potentially informing treatment strategies.

INTRODUCTION

Autoimmune diseases are disorders in which the immune system attacks healthy cells and tissues. These conditions can affect many different organ systems with diverse symptoms. One common feature of many autoimmune diseases is the occurrence of flares, also called relapses. Relapses are episodes of increased disease severity. Autoimmune diseases are thus often characterized by relapses and remissions in which symptoms appear and then subside. Examples include multiple sclerosis (MS),[1] rheumatoid arthritis,[2] inflammatory bowel disease[3] (IBD), lupus,[4] myasthenia gravis,[5] and psoriasis.[6] There is also evidence for relapsing-remitting or cyclical Graves' disease,[7,8] although the underlying physiological mechanisms are not fully understood.[9]

Several factors can trigger a flare, including infections, stress and exposure to certain drugs or other environmental factors.[10–12] It is believed that these triggering factors may disrupt the balance between immune effector cells and regulatory cells, causing an enhanced autoimmune attack.[13,14]

The rate of relapses varies between autoimmune diseases. In MS, one of the best studied diseases, relapse rate averages about 0.6/year.[15]

The development of autoimmune diseases and flares is influenced by genetic and environmental factors, but the specific mechanisms underlying these processes are not yet fully understood.[16] A better understanding of the underlying mechanisms that contribute to flares could inform treatment strategies aimed at reducing relapse rates. Therefore, it is important to identify potential unifying mechanisms that could explain the occurrence of flares across different autoimmune diseases.

Mathematcial studies on autoimmune flares have focused on models of the immune system that give rise to oscillatory flare dynamics.[17–19] Flares in these models thus have a defined period. However, this periodicity is at odds with clinical data in which relapses do not seem to have a defined period.[15,20] Moreover, these models typically do not incorporate the impact of environmental triggers on flare occurrence, which have been suggested to be major contributing factors to flare events in autoimmune diseases.[21,22]

Here we hypothesize that flares result from excitable dynamics in the immune system. Excitability is a property in which a triggering event causes a large pulse of activity that returns to a locally stable baseline. Unlike oscillatory models, each new pulse requires a new triggering event, and flares thus appear stochastically with no defined period. We present a minimal model of immune effector and regulatory cells which shows excitability. Flares are triggered by factors such as stress and infection that push immune activity beyond a threshold. We compare the model predictions to datasets on MS relapses, and describe relapse changes during pregnancy. The model suggests that mild interventions in certain key parameters can profoundly reduce the relapse rate, offering directions for future treatment strategies.

[1]Department Molecular Cell Biology, Weizmann Institute of Science, Rehovot 76100 Israel
[2]Lead contact
*Correspondence: uri.alon@weizmann.ac.il
https://doi.org/10.1016/j.isci.2023.108084

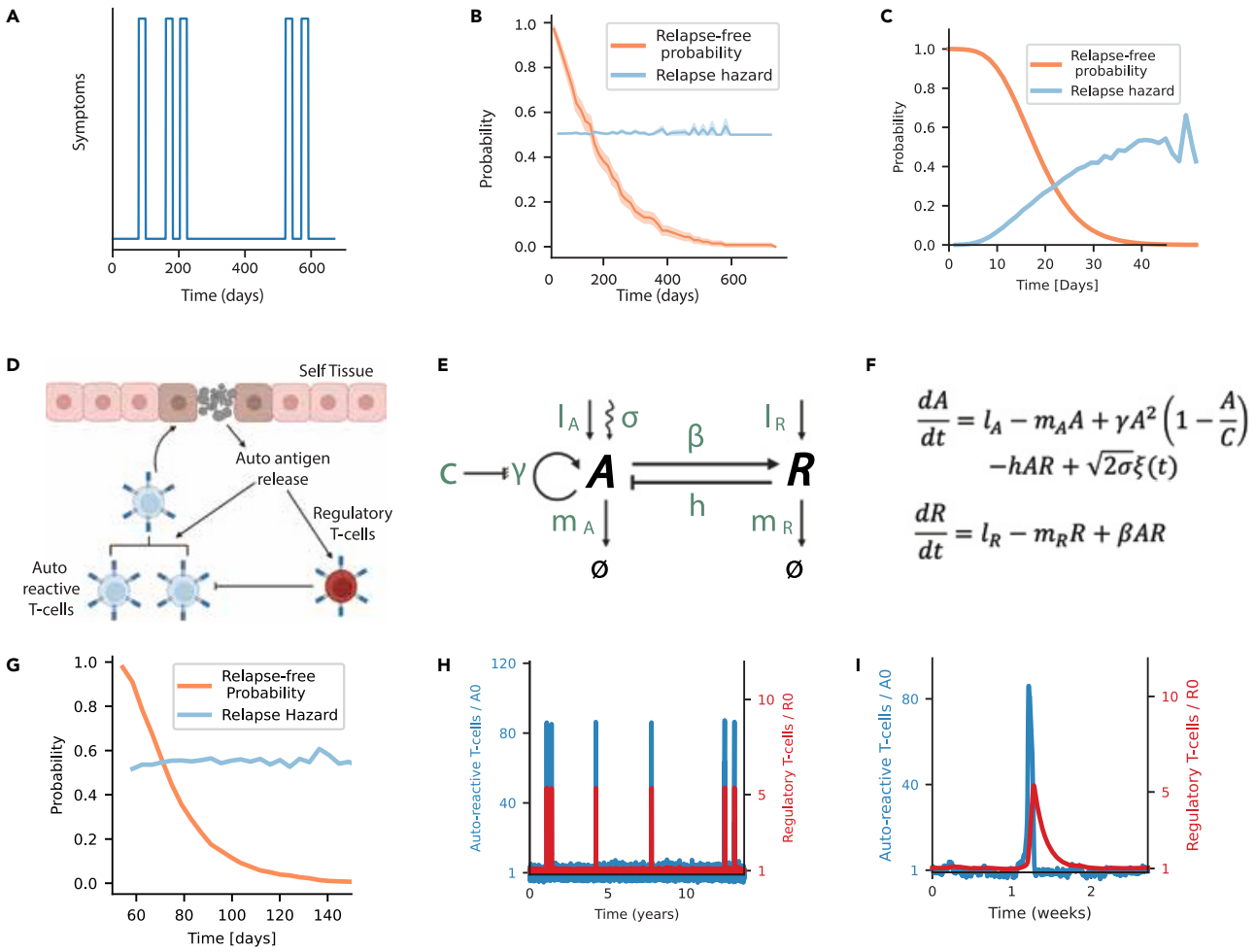

Figure 1. Excitable model of the immune system shows stochastic flares

(A) A time course of a patients' symptoms taken from the MSOAC database.

(B) Relapse-free times and relapse hazard rates of all patients in the database that have precise relapse dates.

(C) Relapse-free survival and hazard for oscillatory behavior from 500 simulations.

(D) Schematic of the relapse model in which autoreactive effector T-cells *A* kill tissue cells, releasing autoantigen that enhances proliferation of *A* and of regulatory cells *R* that inhibit *A*.

(E) Circuit diagram of relapse model.

(F) Model equations. For definition of the parameters used in E and F see STAR Methods.

(G) Relapse-free survival and hazard in the relapse model from 1000 simulations.

(H) Stochastic simulations show spike-like flares of *A*.

(I) Zoom-in on a single flare with a rise in *A* followed by a rise in *R*, a decline in *A* and a slower decline of *R*.

RESULTS

Relapse statistics in MS suggest stochastic excitability rather than oscillatory dynamics

To investigate the temproal distribution of relapses we analyzed the Multiple Sclerosis Outcome Assessments Consortium (MSOAC) database.[23] This database contains records of patients in placebo arms of clinical trials done in MS patients from the year 2012 onwards. The database contains 139 relapses with exact dates from 31 patients with relapsing-remitting MS (Table Relapse Events - Clinical Data in the deposited data). A time course for one patient is shown in Figure 1A. The relapse-free survival probability (see STAR Methods) is exponential, with a mean of 191 $\pm$ 10 days (Figure 1B). In other words, the probability of a relapse per unit time, known as the relapse hazard, is roughly constant in time.

This analysis precludes an oscillatory mechanism of relapses, which would have a specific inter-relapse time, so that the relapse free survival is sigmoidal and drops around a specific interval duration (Figure 1C). The observed exponential distribution of relapse-free survival times does not have such a typical interval period. This observation, together with the spike-like nature of the relapses, suggest a mechanism in which stochastic effects cause flares in an excitable system.

An excitable model of the immune system shows stochastic flares

We developed a minimal mathematical model of autoimmune flares based on well characterized immune interactions. Our goal was to investigate whether a simple model of immune activity could exhibit excitability, characterized by the ability to produce stochastically occurring flares of activation with a constant probability per unit time, and a refractory period.

We focus on autoimmune effector T-cells, which we denote as *A*. These CD4 and CD8 T-cells can target and attack healthy tissue (Figure 1D). This attack releases autoantigens, which raise the proliferation rate of the effector cells.[16,24] The autoantigens also induce proliferation of regulatory T-cells, such as Foxp3+ Tregs, which we denote as *R*.[25] These regulatory cells suppress the effector cells.[16,26]

We model these interactions using differential equations for the rate of change of *A* and *R* (Figures 1E and 1F). We explored various mathematical models based on the known interactions between these two cell types and ultimately arrived at a simple model that exhibited strong excitability (see STAR Methods for alternative models).

This model, which we call the *relapse model*, is based on the production and removal of effector T-cells (A), whose proliferation rate is proportional to autoantigen levels. The autoantigen level is proportional to A becuase an autoimmune response releases autoantigen, resulting in an autocatalytic proliferation of *A* that goes as A^2. To avoid singularities in which *A* goes to infinity, we employ a carrying capacity term in which proliferation drops to zero when *A* reaches a maximal level *C*.[27–29] This carrying capacity can be due to the limited number of naive cells with the required reactivity, their maximal clone size determined in the lymph node,[30] and limitations of physical space and growth factors.

The effector T-cells *A* are inhibited by regulatory T-cells *R* as described by a negative 'mass-action' term proportional to the product *AR*. This term models effects which require proximity of *A* and *R* cells, including direct killing by contact or local consumption of IL2 by *R* cells.[31,32] Under normal conditions, regulatory T-cells are produced and eliminated at baseline levels, meaning that the number of cells in a given lymph node remains relatively stable. However, in the presence of autoantigen, their replication rate increases, leading to an increase in the number of regulatory T-cells, represented by a term proportional to AR. Our model assumes that the maintenance of tolerance toward autoreactive T-cells at baseline levels is mainly driven by the baseline levels of regulatory T-cells, rather than the natural turnover of these cells.[33]

To model stochastic activation of the effector T-cells we add a noise term to the equation for *A*. The noise term is essential to trigger the flares. The noise term can represent at least two known factors that enhance the rate of relapses. The first is infections which can activate autoimmune responses in susceptible individuals.[34] This is effectively an increase in *A* production rate. The second is stress, which acts through endocrine and neuronal pathways to affect the immune system.[35,36]

We note that a noise term can also be added to the *R* equation, although this does not result in qualitative changes to our conclusions (see STAR Methods).

Simulations of the resulting differential equations show stochastic flares (Figures 1G and 1H). In each flare, *A* rises sharply, followed by a rise in *R* which inhibits *A* (Figure 1I). The flare ends with an exponential decrease of *R*. A new flare is formed when noise triggers the excitable system again. The relapse model shows flares whose timing is exponentially distributed (Figure 1G), as observed in the MS dataset.

The dynamics produced by the relapse model qualitatively agree with studies that show an increase of T helper cells during relapses and an enhanced presence of regulatory T-cells during remission.[37,38]

Our findings suggest that the relapse model, which captures key immunological interactions, can exhibit excitability and generate flares or relapses that resemble those observed in MS and other autoimmune diseases.

Rate and shape of flares are governed by specific model parameters

To understand the relapse model we employ a phase portrait analysis using nullclines[39] (Figure 2A). Each nullcline represents the steady state of one variable when holding the other variable fixed. This decomposes the feedback loop into two arms[40,41]: one arm in which *A* induces *R*, and the other arm in which *R* inhibits *A*. The crossing points of the two nullcline curves are the fixed points of the system.

The first nullcline ($\frac{dR}{dt} = 0$, in red) shows how the *R* steady state monotonically rises with *A*. The second nullcline ($\frac{dA}{dt} = 0$, in blue) has an inverse-N shape. Inhibition of *A* by *R* explains the leftmost descending arm of this nullcline. When *R* is at intermediate levels, autostimulation of *A* dominates over its inhibition by *R*, which results in an ascending curve. Finally, at high *A*, effector cell production decreases as the population approaches its carrying capacity, resulting in another descending arm of the nullcline. The inverse-N shape of the *A* nullcline is important for excitability.[42]

Excitability occurs when the nullclines cross in the left declining segment of the N-shaped nullcline. This provides a single stable fixed point, representing a physiological state in which autoimmune effector T-cells are present and held in check by regulatory T-cells. The presence of such autoimmune T-cells in the healthy population which can target cells involved in autoimmune diseases such as MS, type 1 diabetes and thyroiditis, has been documented.[33,43]

When noise - including infection or stress - pushes the system away from the stable fixed point and across the ascending branch of the *A* nullcline, the system enters the excitable region (point 1 in Figure 2B). Effector cells *A* grow rapidly due to the A^2 term, and reach a value close to their carrying capacity *C* (point 2). This induces growth of *R* cells (point 3) which inhibits the *A* cells until they return to the first descending branch of the *A* nullcline (point 4). Finally, *R* cells decline and the system returns to baseline (point 5).

The dynamics of a flare is shown in Figures 2B and 2C, with key timepoints labeled for clarity.

Noise thus triggers flares by pushing the system across a threshold. To calculate the rate of flares analytically we used the Kramer approach. This method involves calculating an effective potential that determines how likely the system is to cross a threshold after being perturbed by noise. The potential difference, or ΔU, represents the potential barrier that the system must overcome in order to start a flare - a large excursion in the phase space that returns to the fixed point. The probability of the system crossing this potential barrier is proportional to $exp\left[-\frac{\Delta U}{\sigma}\right]$, where σ is the amplitude of the noise. In other words, the larger the potential difference and the smaller the noise, the less likely

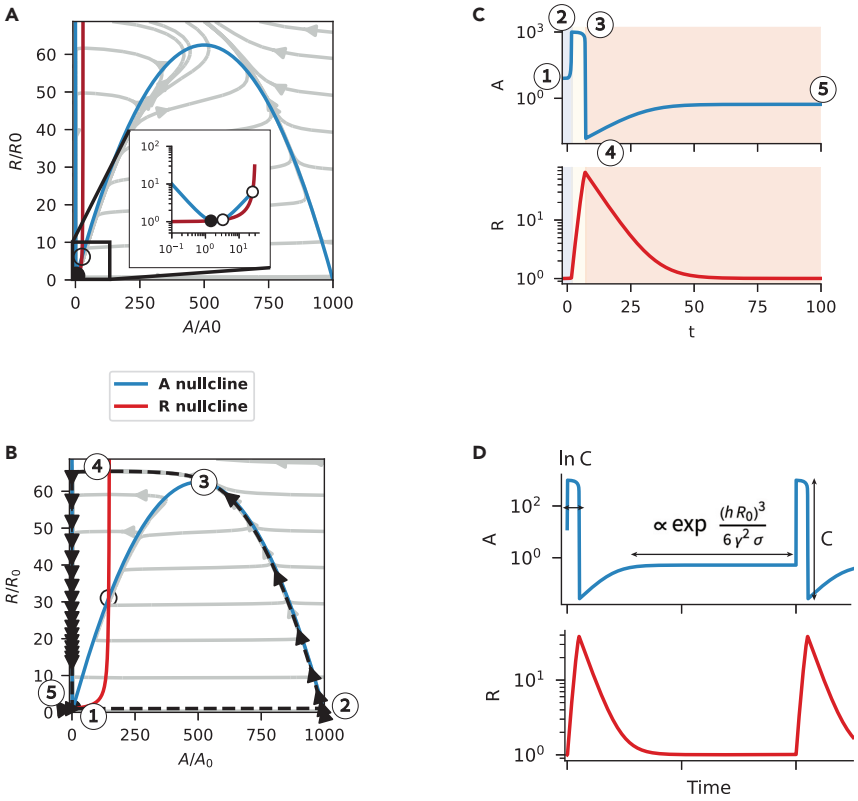

Figure 2. Analysis of noise-induced flares

(A) Phase portrait of the excitable system, showing nullclines, with fixed points shown in the inset.

(B) Flare trajectory in phase space.

(C) Temporal evolution of autoimmune and regulatory T-cells during a flare. Numbers in circles indicate timepoints that correspond to the numbers in (B).

(D) Parameter dependence of flare duration, amplitude and inter-flare interval. Model parameters groups are: $B = 0.001$, $G = 0.25$, $D = 0.15$, $C = 1000$, in units where flare duration is two weeks, and flare rate is 1/year (see STAR Methods).

the system is to cross the barrier and generate a relapse. The effective potential and potential difference are therefore key factors that determine the rate and shape of flares in our model. An exact solution is provided in STAR Methods.

This barrier-crossing dynamic produces an exponentially distributed flare spacings, with mean flare rate

(1) $r \propto exp\left[\frac{hR_0 I_A}{\gamma\sigma} - \frac{(hR_0)^3}{6\gamma^2\sigma}\right]$ (Figure 2D, STAR Methods).Where $R_0 = \frac{I_R}{m_R}$ is the baseline level of the regulatory T cells. The standard deviation of the flare timing is equal to the mean since the flare timing distribution is exponential.

The model parameters also affect the shape of each flare (see STAR Methods - relapse shape and duration for details). The flare amplitude is proportional to the effector cell carrying capacity C. Flare duration is proportional to $ln\ C$, due to the super-exponential growth of A during each flare (Figure 2C). After the flare, effector T-cells drop below baseline and regulatory cells are above baseline, making it unlikely to have another relapse. This is a refractory period whose duration is proportional to $\frac{ln\ C}{m_R}$. The refractory period is typically much shorter than the inter-spike time, and thus the exponential relapse-free survival distribution is a good approximation at times longer than the refractory period.

We provide a table of estimated parameters in terms of dimensionless parameter groups (Table S1). T-cell lifetimes (both effector and regulatory) are on the order of days. Since flares entail sufficient damage to cause symptoms, we assume a carrying capacity a thousand times larger than baseline, $C = 10^3$ to allow for large spikes[44] - the results remain qualitatively the same for values of C that are $C = 10$ or larger. In the simulations we use dimensionless effector cell reactivity $G = \frac{\gamma A_0}{hR_0} = 0.25$ where the steady state is A_0 and R_0 for A and R cells respectively.

The range of parameters that provides excitability is large (Figure 3A)- a range of several orders of magnitude for each parameter around the parameters used for Figures 2A–2C- as described in more detail in the next section.

Notably, the model exhibits strong flares despite the fact that autoreactive T-cells and regulatory T-cells have similar turnover rates. This is unlike standard models of excitable systems such as the Fitzhugh-Nagumo model which describes, for example, neuronal spikes. These standard models depend on separation of turnover times where the fast variable can rise before the slow inhibitory variable can overtake it. The reason that the present model shows strong flares is the autostimulation in the A equation ($\frac{dA}{dt} \sim A^2$). This causes a super-exponential rise in autoreactive T-cells - a finite time singularity which is prevented by their carrying capacity. The super-exponential rise outruns the rise in regulatory cells. The stark nature of the flare can be seen in the nearly horizontal dynamical arrows in Figure 2A, which effectively creates a separation of timescales.

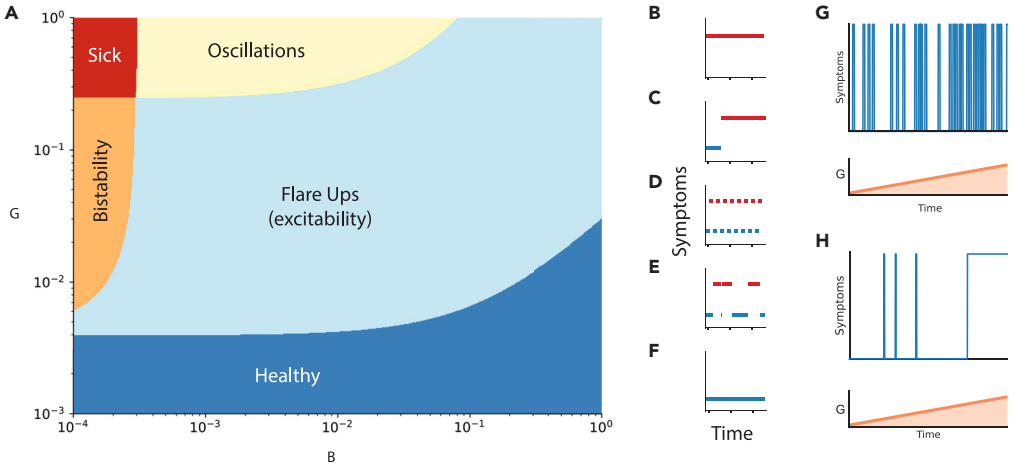

Figure 3. Phase diagram of the model and transitions to progressive disease

(A) Phase diagram of the different regimes of behavior as a function of the auto-stimulatory parameter G γ and regulatory stimulation parameter B β. See Figure S2 in the supplementary information for additional phase diagrams.

(B–F) Qualitative time series for the different regimes: B) Single sick state.

(C) Bistability of the healthy and sick states. D) Oscillations between healthy and sick states.

(E) Flare ups.

(F) Single healthy state.

(G) simulations with increasing gamma showing onset of excitable flares which transition to rapid oscillations.

(H) simulations with increasing gamma showing onset of excitable flares which transition to chronic activation. Dimensionless parameters (see STAR Methods): $G(t) = 0.25 + 5 \cdot 10^{-6} t, B = 5 \cdot 10^{-3}$ in G, $G(t) = 0.03 + 1.4 \cdot 10^{-5} t, B = 3 \cdot 10^{-4}$ in H.

Transitions between flares and chronic disease

MS patients can transition from a relapse-remitting disease to a more chronic form called secondary progressive disease in which disability becomes progressively worse. To understand such a transition, we consider the possible behaviors of the model when parameters change.

We depict these behaviors in a phase diagram in Figure 3A. Excitability occurs in a wide region of parameters. Regimes other than excitability occur when parameter thresholds are crossed. When the autoantigen stimulation parameter γ is very low the model shows a monostable situation with no flares - corresponding to a healthy state. When γ is very high the model shows a chronically sick state with constant high autoimmune activation - similar to chronic autoimmune disease states. A region of bistability occurs when regulatory T-cells are weakly triggered by antigen (low β) - this effectively corresponds to a chronic autoimmune disease once triggered. Finally, oscillations (instead of excitability) occur in a region of parameter space with high γ and intermediate β (Figure 3).

One pathway from health to flares to chronic state may be a gradual increase in the stimulation parameter γ. This increase may be due to epitope spreading in which damage to a tissue causes the establishment of effector cells (T cells and B cells) to a wider range of antigens than before the damage.[45–47] In principle, every flare has a chance to increase γ, making the system more auto-stimulatory. A trajectory of increasing γ can transition between the healthy part of the phase diagram, through the excitable region, and finally to a bistable or oscillatory region (depending on β) (Figures 3G and 3H). In the oscillatory regime, the spikes of the oscillation occur at a period determined by the refractory period, and thus may resemble a chronic autoimmune attack in which each spike is followed closely by another. Both the bistable and oscillatory endpoints may thus point to a progressive increase in disability.

Model predicts the changes in relapse rate in pregnancy and postpartum

To test the model, we consider the changes in autoimmune relapse rates during pregnancy and the postpartum period. During pregnancy, the immune system undergoes changes that suppress harmful responses to the fetus, leading to a decrease in the severity of some autoimmune disorders. This is due to an increase in regulatory T-cells and anti-inflammatory cytokines.

Data on the relapse rate of MS shows a decline during pregnancy followed by a rebound in the first three months after delivery,[48] Figure 4A.

To compare this to the model, we obtained data on the temporal dynamics of lymphocytes during pregnancy from the Clalit dataset on about 500,000 pregnancies.[49] This cross-sectional dataset includes 1.5 million lymphocyte counts averaged over each week of pregnancy and 80 weeks postpartum (Figure 4B). Mean lymphocyte counts decrease during pregnancy and increase after delivery, returning to baseline (pre-pregnancy) level after about 60 weeks.

We reasoned that lymphocyte counts can serve as an approximate measurement for A_0, the baseline level of effector T-cells. We furthermore assumed that the combined effect of decrease in total amount of lymphocyte count and the relative expansion of regulatory T-cells[44]

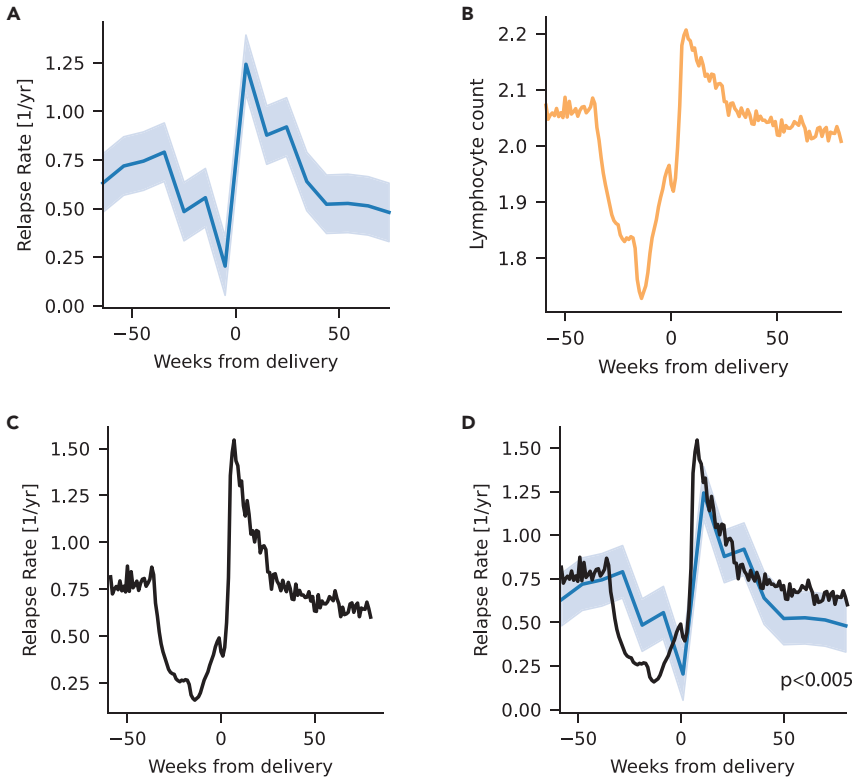

Figure 4. Model predicts MS relapse rate variation in pregnancy and postpartum based on lymphocyte counts

(A) MS relapse rate averaged over three month periods from Vukusic et al.

(B) Lymphocyte count blood tests from the Clalit dataset (n = 1.4 million tests) averaged over each week from 60 weeks before delivery to 80 weeks after.

(C) Relapse rate computed from model Equation 1 with $r_{baseline}$ = 0.6/year and q = 10.

(D) Overlay of computed and measured relapse rates. P value (p) represents the statistical significance of agreement between the model prediction and observed data.

can be approximately described by constant levels of R_0. We then used Equation 1 to calculate the relapse rate relative to baseline. The relation between relapse rate r and the relative change in lymphocyte levels ϵ can be written as $r = r_{baseline}e^{q\epsilon}$ with a single fit parameter q, using $r_{baseline}$ = 0.6/year. We find that this equation captures the observed dynamics of the normalized relapse rate well with $q = 10 \pm 4$ (R = 0.82, p < 0.005).

Model suggests parameter modulations to reduce the relapse rate

To explore potential targets for intervention, we asked which parameters of the model affect the relapse rate most strongly. For this purpose we evaluated the sensitivity with respect to each parameter in the mathematical model. Sensitivity of relapse rate r to a given parameter q is $\frac{d\ log\ r}{dq}$ (see STAR Methods), which is roughly equal to the percent change in relapse rate for a 1% change in the parameter. We used the estimated parameters from the pregnancy dataset as the baseline system parameters. Schematic and quantitive depiction of the sensitivities are shown in Figure 5.

We found that most parameters had high sensitivity, with a 1% change in parameters resulting in a greater than 10% change in the relapse rate. The parameters with the largest effect were the baseline level of regulatory T-cells (R_0), their inhibitory effect (h), and the autostimulation parameter γ.

Although the carrying capacity (C) and the activation rate of regulatory cells (β) are included in our model, they have negligible effect on the relapse rate.The natural turnover rate of autoreactive cells (m_A) also had negligible effects within the present parameter range.These parameters only affected the shape and amplitude of each relapse.

The high sensitivity for certain parameters is optimistic for treatment strategies. Suppose that our aim is to reduce relapse rate by a factor of 100, which guarantees lack of relapses because it converts the ~1/year relapse rate to less than 1/lifespan. To achieve this, one need only have a 15% decrease of γ, or a 22% increase in either l_R or h. A combination of parameter changes would require even smaller effects, such as changing both l_R and h by 11%. Thus, our findings provide hope for developing effective treatments that target immune system parameters related to the relapse rate.

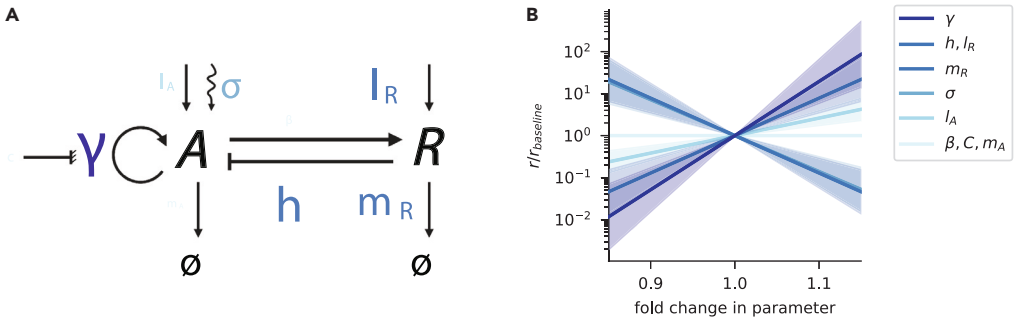

Figure 5. Certain parameter changes can strongly reduce the relapse rate

(A) Parameters in the circuit, letter size indicates the sensitivity of relapse rate to each parameter.

(B) Relative change in relapse rate for a relative change in each parameter. Note the logarithmic y axis. Baseline parameter group is q = 10.

The immune system is a complex system that requires fine-tuning of its parameters for proper function. While the model allows for a large variety of inter-relapse times, in reality, only a limited range of parameter combinations produce relapse rates that are characteristic of an active disease. Therefore, the specific combination of parameters that is required for disease activity is likely to lie within a small region of the parameter space that is consistent with the fine-tuned parameters of the immune system, which presumably were selected to provide proper pathogen response.

DISCUSSION

We present an excitable mechanism for flares in autoimmune diseases based on a minimal model of the adaptive immune system. The model describes interactions between autoimmune cells and inhibitory regulatory cells, and shows robust excitatory spikes that occur at random times. We present evidence based on a medical dataset that flares in MS are not oscillatory but rather have an exponential inter-flare time distribution, which is explained by the presented model. The model can explain the decline of MS relapse during pregnancy and the postpartum surge in relapses based on longitudinal lymphocyte measurements. It also indicates which interactions might serve as targets to reduce relapse rates. It predicts that mild intervention in certain regulatory T cell parameters can have large beneficial effects on reducing relapse rate, offering insight to potential treatment strategies.

The present model indicates that a relapse is triggered when autoreactive cells levels are raised beyond a threshold. The dynamics show a rapid rise in autoreactive activity, reaching close to its carrying capacity, followed by a rise in regulatory T-cell activation which shuts off the flare. Several factors may be responsible for triggering the flare, and these are described as noise in the model that affects autoimmune activation stochastically. One key factor is infections, which are known to often occur before flares in autoimmune diseases such as MS,[50] lupus,[4] and other diseases. Other factors include stress, which has pleiotropic effects on the adaptive immune system and which can incite autoimmune flares.[51,52]

Excitable systems have been extensively studied in neurons, and their dynamics have been understood using canonical models like the Fitzhugh-Nagumo model.[53–55] Typically, strong flares in these models depend on having a fast variable and a slow variable with strong separation of timescales.[56] The present model provides strong flares even without explicit separation of timescales between the two equations, due to a strong autocatalysis of the autoimmune cells. This results in similar timescales near the stable fixed point, but very fast dynamics for A when the spike is triggered. Indeed, autoimmune cells and regulatory cells are expected to have similar turnover times.

The present model differs from previous mathematical models that treat autoimmune flares as oscillations, because it treats flares as an excitable system. Oscillatory models predict a periodic appearance of flares, or if they include noise, a periodic appearance with some stochastic variation, whereas in reality flares usually do not seem to have a characteristic period, as we find in MS data. The present model predicts an exponential distribution of inter-flare times (at times longer than the refractory period), provided that flares are triggered by a stochastic process with essentially constant probability per unit time.

We note that oscillatory dynamics in other (non-autoimmune) diseases have been documented.[55] The present model has a region of parameter space in which it has oscillatory solutions.

The model is agnostic to the precise antigen and target tissue, and thus may potentially apply to a wide range of autoimmune diseases with flares; these include SLE (lupus), rheumatoid arthritis, inflammatory bowel syndrome, psoriasis and Graves' disease.

One may speculate that additional diseases may have a currently unknown flare dynamic. One such disease is type 1 diabetes.[57] This disease has a 'honeymoon phase' in which initial treatment often causes glucose control to return for a few months, followed by relapse of the disease. This may indicate flare dynamics. It would be interesting to explore whether chronic diseases such as Hashimoto's thyroiditis also have flare dynamics during their subclinical phase.

The duration of each flare-up in the model is controlled by the logarithm of the carrying capacity of autoreactive cells, $ln\ C$. This suggests that changes in the carrying capacity over time, such as epitope spreading that increases C or immune decline that reduces C, would have a relatively minor effect on flare duration due to the logarithmic dependence.

The model might also provide insight into the transition from relapsing-remitting disease to chronic (secondary progressive) disease as occurs in MS. This transition may be due to slow changes in the model parameters that cross between the excitable regime and the bistable or chronic regime in which autoimmunity is constantly active. These slow changes in parameters may occur with the number and severity of relapses. For example, a rise in γ, the autoantigen-driven amplification of autoreactive T-cells, can cause a shift to chronic autoimmunity. This may occur due to increasing autoantigen-sensitivity that occurs with an increasing number of flares due, for example, to antigen spreading.[45–47]

The model can potentially also address changes in autoimmune flares with age. Aging generally increases memory Tregs and decreases memory effector cells,[58] together with declining total lymphocytes. The model therefore predicts a decline in relapse rate with age which is indeed reported in MS.[59]

The model offers insights into potential therapeutic targets for treating relapsing-remitting autoimmune diseases. First, our findings suggest that enhancing the production and suppressive effect of regulatory T cells (Tregs) is a promising target. This can be achieved through various interventions, such as IL-2 therapy, which boosts Treg production and activity,[60–63] and immune checkpoint inhibitors like CTLA-4 agonists,[64] which enhance Treg function.

Second, the model highlights the significance of targeting the sensitivity of autoreactive T cells to autoantigen. Strategies that modulate this sensitivity are predicted to reduce flare frequency. Relevant interventions include anti-CD3 antibodies[65–67] and immune checkpoint inhibitors.[64]

The model also bears on effects of cancer immunotherapies on autoimmune diseases. For example, immune checkpoint treatments used for cancer therapy, while effective in enhancing immune attack on cancer cells, can have the side effect of inadvertently impairing Treg function, leading to an increased risk of multiple autoimmune diseases.[68] The model may also be adapted to analyze immune attack on cancer cells, raising the possibility that such attack is pulsatile in nature rather than continuous. The parameter modulations found here to reduce autoimmune relapse rate may be used in reverse as potential targets to increase the rate of flares of beneficial immune attack on cancer cells.

An essential feature of the present model includes intertwined negative and positive feedback loops. This motif is prevalent in other models of the immune response. For example, a recent model for COVID-19 by Tretter et al. highlights positive and negative feedback loops in disease progression.[69] More generally, autoimmune pulses might be due at their core to a pulsatile design of the anti-pathogen response, with an autocatalytic phase that ensures a strong response and a shutdown phase that prevents excessive immune damage. Investigating the shared features of autoimmune flares and pathogen response may further our understanding of the immune system.

In summary, we presented a mechanism in which the interplay of autoimmune and regulatory cells can cause robust flares triggered stochastically by factors such as infection and stress. The model helps to quantitatively predict how changes in the adaptive immune system translate to changes in relapse frequency. It points to several key interactions as potential targets for reducing the relapse rate - even small modulation of regulatory T cell production, removal or activity is predicted to have strong effects on relapse rate. Such quantitative approaches can inform treatment strategies.

Limitations of the study

The present model simplifies the complex interactions in the immune system to highlight fundamental dynamics of autoimmune diseases. While this approach is insightful, it disregards intricate details that could impact real-world scenarios. Additionally, the current parameter values are based on available data and assumptions, potentially missing the full spectrum of patient variability. The model's linear response assumptions might not encompass the nonlinear nature of immune interactions. External influences, such as genetics, environment, and co-existing conditions, are not accounted for in our model. Furthermore, our predictions lack direct clinical validation and may not hold in all disease scenarios. While our model explains pregnancy-related MS relapses, it does not capture the entirety of hormonal and immunological changes. Lastly, while applicable to diverse autoimmune diseases, our model may not encompass the complete scope of these complex disorders.

STAR★METHODS

Detailed methods are provided in the online version of this paper and include the following:

- KEY RESOURCES TABLE
- RESOURCE AVAILABILITY
  - Lead contact
  - Materials availability
  - Data and code availability
- METHOD DETAILS
  - Relapse-free probability and relapse hazard curves from MSOAC database
  - Model equations
  - First passage time
  - Rationale for noise in the A equation
  - Relapse Shape and Duration
  - Pregnancy
  - Sensitivity analysis

- Alternative models
- Dynamics limited by self-tissue

SUPPLEMENTAL INFORMATION

Supplemental information can be found online at https://doi.org/10.1016/j.isci.2023.108084.

ACKNOWLEDGMENTS

This project was funded by the European Research Council (ERC) under the European Union's Horizon 2020 research and innovation program (grant agreement No 856487). Data acquisition was approved by the Clalit Helsinki committee RMC-1059-20. The authors thank the investigators from the Multiple Sclerosis Outcome Assessment Consortium (MSOAC) Placebo Database for providing data used in this study.

AUTHOR CONTRIBUTIONS

Conceptualization: Y.L., A.B., T.M., A.M., and U.A.; Methodology: Y.L, A.B., A.M., and U.A.; Software: Y.L. and A.M.; Formal Analysis: Y.L. and A.M.; Data Curation: Y.L.; Writing – Original Draft: Y.L. and U.A.; Writing – Review and Editing: Y.L., A.B., T.M., A.M., and U.A.

DECLARATION OF INTERESTS

The authors declare no competing interests.

Received: May 3, 2023
Revised: August 4, 2023
Accepted: September 25, 2023
Published: September 27, 2023

REFERENCES

1. Filippi, M., Bar-Or, A., Piehl, F., Preziosa, P., Solari, A., Vukusic, S., and Rocca, M.A. (2018). Multiple sclerosis. Nat. Rev. Dis. Prim. *4*, 43.
2. Bykerk, V.P., Lie, E., Bartlett, S.J., Alten, R., Boonen, A., Christensen, R., Furst, D.E., Hewlett, S., Leong, A.L., Lyddiatt, A., et al. (2014). Establishing a Core Domain Set to Measure Rheumatoid Arthritis Flares: Report of the OMERACT 11 RA Flare Workshop. J. Rheumatol. *41*, 799–809.
3. Zhang, Y.Z., and Li, Y.Y. (2014). Inflammatory bowel disease: Pathogenesis. World J. Gastroenterol. *20*, 91–99.
4. Fernandez, D., and Kirou, K.A. (2016). What Causes Lupus Flares? Curr. Rheumatol. Rep. *18*, 14.
5. Wang, L., Zhang, Y., and He, M. (2017). Clinical predictors for the prognosis of myasthenia gravis. BMC Neurol. *17*, 77.
6. Gordon, K.B., Feldman, S.R., Koo, J.Y.M., Menter, A., Rolstad, T., and Krueger, G. (2005). Definitions of Measures of Effect Duration for Psoriasis Treatments. Arch. Dermatol. *141*, 82–84.
7. Fan, W., Tandon, P., and Krishnamurthy, M. (2014). Oscillating hypothyroidism and hyperthyroidism – a case-based review. J. Community Hosp. Intern. Med. Perspect. *4*, 25734. https://doi.org/10.3402/jchimp.v4.25734.
8. Martins, L.C., Coutinho, A.R., Jerónimo, M., Caetano, J.S., Cardoso, R., Dinis, I., and Mirante, A. (2016). Autoimmune alternating hyper- and hypo-thyroidism: a rare condition in pediatrics. Endocrinol. Diabetes Metab. Case Rep. *2016*, 150131.
9. Takasu, N., and Matsushita, M. (2012). Changes of TSH-Stimulation Blocking Antibody (TSBAb) and Thyroid Stimulating Antibody (TSAb) Over 10 Years in 34 TSBAb-Positive Patients with Hypothyroidism and in 98 TSAb-Positive Graves' Patients with Hyperthyroidism: Reevaluation of TSBAb and TSAb in TSH-Receptor-Antibody (TRAb)-Positive Patients. J. Thyroid Res. *2012*, 1–11.
10. Waubant, E., Lucas, R., Mowry, E., Graves, J., Olsson, T., Alfredsson, L., and Langer-Gould, A. (2019). Environmental and genetic risk factors for MS: an integrated review. Ann. Clin. Transl. Neurol. *6*, 1905–1922.
11. Kamel, F.O. (2019). Factors involved in relapse of multiple sclerosis. J. Microsc. Ultrastruct. *7*, 103–108.
12. Xie, Y., Tian, Z., Han, F., Liang, S., Gao, Y., and Wu, D. (2020). Factors associated with relapses in relapsing-remitting multiple sclerosis: A systematic review and meta-analysis. Medicine (Baltim.) *99*, e20885.
13. Kuchroo, V.K., Ohashi, P.S., Sartor, R.B., and Vinuesa, C.G. (2012). Dysregulation of immune homeostasis in autoimmune diseases. Nat. Med. *18*, 42–47.
14. Herman, A.E., Freeman, G.J., Mathis, D., and Benoist, C. (2004). CD4+CD25+ T Regulatory Cells Dependent on ICOS Promote Regulation of Effector Cells in the Prediabetic Lesion. J. Exp. Med. *199*, 1479–1489.
15. Nicholas, R., Straube, S., Schmidli, H., Schneider, S., and Friede, T. (2011). Trends in annualized relapse rates in relapsing–remitting multiple sclerosis and consequences for clinical trial design. Mult. Scler. *17*, 1211–1217.
16. Rosenblum, M.D., Remedios, K.A., and Abbas, A.K. (2015). Mechanisms of human autoimmunity. J. Clin. Invest. *125*, 2228–2233.
17. Iwami, S., Takeuchi, Y., Miura, Y., Sasaki, T., and Kajiwara, T. (2007). Dynamical properties of autoimmune disease models: tolerance, flare-up, dormancy. J. Theor. Biol. *246*, 646–659.
18. Velez de Mendizabal, N., et al. (2011). Modeling the effector - Regulatory T cell cross-regulation reveals the intrinsic character of relapses in Multiple Sclerosis. BMC Syst. Biol. *5*, 1–15.
19. Zhang, W., Wahl, L.M., and Yu, P. (2014). Modeling and analysis of recurrent autoimmune disease. SIAM J. Appl. Math. *74*, 1998–2025.
20. Bordi, I., et al. (2013). A Mechanistic, Stochastic Model Helps Understand Multiple Sclerosis Course and Pathogenesis. Int. J. Genomics *1–10*.
21. Vollmer, T. (2007). The natural history of relapses in multiple sclerosis. J. Neurol. Sci. *256*, S5–S13.
22. Kalincik, T. (2015). Multiple Sclerosis Relapses: Epidemiology, Outcomes and Management. A Systematic Review. Neuroepidemiology *44*, 199–214.
23. Rudick, R.A., LaRocca, N., and Hudson, L.D.; MSOAC (2014). Multiple Sclerosis Outcome Assessments Consortium: Genesis and initial project plan. Mult. Scler. *20*, 12–17.
24. Kravitz, M.S., and Shoenfeld, Y. (2006). Autoimmunity to protective molecules: is it the perpetuum mobile (vicious cycle) of autoimmune rheumatic diseases? Nat. Clin. Pract. Rheumatol. *2*, 481–490.
25. Jiang, H., and Chess, L. (2006). Regulation of Immune Responses by T Cells. N. Engl. J. Med. *354*, 1166–1176.
26. Theofilopoulos, A.N., Kono, D.H., and Baccala, R. (2017). The multiple pathways to autoimmunity. Nat. Immunol. *18*, 716–724.
27. Huang, H., Sikora, M.J., Islam, S., Chowdhury, R.R., Chien, Y.H., Scriba, T.J., Davis, M.M., and Steinmetz, L.M. (2019). Select sequencing of clonally expanded CD8 $^{+}$ T cells reveals limits to clonal expansion. Proc. Natl. Acad. Sci. USA *116*, 8995–9001.
28. Arias, C.F., Herrero, M.A., Acosta, F.J., and Fernandez-Arias, C. (2017). Population mechanics: A mathematical framework to study T cell homeostasis. Sci. Rep. *7*, 9511.

29. Zhou, X., Franklin, R.A., Adler, M., Jacox, J.B., Bailis, W., Shyer, J.A., Flavell, R.A., Mayo, A., Alon, U., and Medzhitov, R. (2018). Circuit design features of a stable two-cell system. Cell *172*, 744–757.e17.
30. Marchingo, J.M., Kan, A., Sutherland, R.M., Duffy, K.R., Wellard, C.J., Belz, G.T., Lew, A.M., Dowling, M.R., Heinzel, S., and Hodgkin, P.D. (2014). Antigen affinity, costimulation, and cytokine inputs sum linearly to amplify T cell expansion. Science *346*, 1123–1127.
31. Sojka, D.K., Huang, Y.H., and Fowell, D.J. (2008). Mechanisms of regulatory T-cell suppression - A diverse arsenal for a moving target. Immunology *124*, 13–22.
32. Wong, H.S., and Germain, R.N. (2018). Robust control of the adaptive immune system. Semin. Immunol. *36*, 17–27.
33. Liu, Z., Gerner, M.Y., Van Panhuys, N., Levine, A.G., Rudensky, A.Y., and Germain, R.N. (2015). Immune homeostasis enforced by co-localized effector and regulatory T cells. Nature *528*, 225–230.
34. Christen, U., and von Herrath, M.G. (2005). Infections and Autoimmunity—Good or Bad? J. Immunol. *174*, 7481–7486.
35. Khansari, D.N., Murgo, A.J., and Faith, R.E. (1990). Effects of stress on the immune system. Immunol. Today *11*, 170–175.
36. Pruett, S.B. (2003). Stress and the immune system. Pathophysiology *9*, 133–153.
37. Frisullo, G., Nociti, V., Iorio, R., Patanella, A.K., Caggiula, M., Marti, A., Sancricca, C., Angelucci, F., Mirabella, M., Tonali, P.A., and Batocchi, A.P. (2009). Regulatory T cells fail to suppress CD4 $^{+}$ T-bet $^{+}$ T cells in relapsing multiple sclerosis patients. Immunology *127*, 418–428.
38. Frisullo, G., Angelucci, F., Caggiula, M., Nociti, V., Iorio, R., Patanella, A.K., Sancricca, C., Mirabella, M., Tonali, P.A., and Batocchi, A.P. (2006). pSTAT1, pSTAT3, and T-bet expression in peripheral blood mononuclear cells from relapsing-remitting multiple sclerosis patients correlates with disease activity. J. Neurosci. Res. *84*, 1027–1036.
39. Strogatz, S.H. (2018). Nonlinear Dynamics and Chaos (CRC Press). https://doi.org/10.1201/9780429492563.
40. Korem Kohanim, Y., Milo, T., Raz, M., Karin, O., Bar, A., Mayo, A., Mendelson Cohen, N., Toledano, Y., and Alon, U. (2022). Dynamics of thyroid diseases and thyroid-axis gland masses. Mol. Syst. Biol. *18*, e10919.
41. Bar, A., Karin, O., Mayo, A., Ben-Zvi, D., and Alon, U. (2023). Rules for body fat interventions based on an operating point mechanism. iScience *26*, 106047.
42. Lindner, B., García-Ojalvo, J., Neiman, A., and Schimansky-Geier, L. (2004). Effects of noise in excitable systems. Phys. Rep. *392*, 321–424.
43. Korem, Y., Milo, T., Raz, M., Karin, O., Bar, A., Mayo, A., Mendelson Cohen, N., Toledano, Y., and Alon, U. (2022). Dynamics of thyroid diseases and thyroid-axis gland masses. Mol. Syst. Biol. *18*, e10919.
44. Sospedra, M., and Martin, R. (2016). Immunology of Multiple Sclerosis. Semin. Neurol. *36*, 115–127.
45. McRae, B.L., Vanderlugt, C.L., Dal Canto, M.C., and Miller, S.D. (1995). Functional evidence for epitope spreading in the relapsing pathology of experimental autoimmune encephalomyelitis. J. Exp. Med. *182*, 75–85.
46. Yu, M., Johnson, J.M., and Tuohy, V.K. (1996). A predictable sequential determinant spreading cascade invariably accompanies progression of experimental autoimmune encephalomyelitis: a basis for peptide-specific therapy after onset of clinical disease. J. Exp. Med. *183*, 1777–1788.
47. Lehmann, P.V., Forsthuber, T., Miller, A., and Sercarz, E.E. (1992). Spreading of T-cell autoimmunity to cryptic determinants of an autoantigen. Nature *358*, 155–157.
48. Vukusic, S., Hutchinson, M., Hours, M., Moreau, T., Cortinovis-Tourniaire, P., Adeleine, P., and Confavreux, C.; Pregnancy In Multiple Sclerosis Group (2004). Pregnancy and multiple sclerosis (the PRIMS study): Clinical predictors of post-partum relapse. Brain *127*, 1353–1360.
49. Bar, A., Mendelsohn-Cohen, N., Yael, K.K., Avi, M., Yoel, T., and Uri, A. (2023). Pregnancy and postpartum dynamics revealed by an atlas of millions of lab tests. Preprint at bioRxiv. https://doi.org/10.1101/2023.05.11.540359.
50. Steelman, A.J. (2015). Infection as an Environmental Trigger of Multiple Sclerosis Disease Exacerbation. Front. Immunol. *6*, 520.
51. Briones-Buixassa, L., Milà, R., Mª Aragonès, J., Bufill, E., Olaya, B., and Arrufat, F.X. (2015). Stress and multiple sclerosis: A systematic review considering potential moderating and mediating factors and methods of assessing stress. Health Psychol. Open *2*, 2055102915612271.
52. Brown, R.F., Tennant, C.C., Sharrock, M., Hodgkinson, S., Dunn, S.M., and Pollard, J.D. (2006). Relationship between stress and relapse in multiple sclerosis: part I. Important features. Mult. Scler. *12*, 453–464.
53. FitzHugh, R. (1955). Mathematical models of threshold phenomena in the nerve membrane. Bull. Math. Biophys. *17*, 257–278.
54. Nagumo, J., Arimoto, S., and Yoshizawa, S. (1962). An Active Pulse Transmission Line Simulating Nerve Axon. Proc. IRE *50*, 2061–2070.
55. Keener, J., and Sneyd, J. (1998). Mathematical Physiology, *8* (Springer).
56. Gerstner, W., Kistler, W.M., Naud, R., and Paninski, L. (2014). Neuronal Dynamics: From Single Neurons to Networks and Models of Cognition (Cambridge University Press).
57. von Herrath, M., Sanda, S., and Herold, K. (2007). Type 1 diabetes as a relapsing–remitting disease? Nat. Rev. Immunol. *7*, 988–994.
58. Rocamora-Reverte, L., Melzer, F.L., Würzner, R., and Weinberger, B. (2020). The Complex Role of Regulatory T Cells in Immunity and Aging. Front. Immunol. *11*, 616949.
59. Tremlett, H., Zhao, Y., Joseph, J., and Devonshire, V.; UBCMS Clinic Neurologists (2008). Relapses in multiple sclerosis are age- and time-dependent. J. Neurol. Neurosurg. Psychiatry *79*, 1368–1374.
60. Furtado, G.C., Curotto de Lafaille, M.A., Kutchukhidze, N., and Lafaille, J.J. (2002). Interleukin 2 Signaling Is Required for CD4+ Regulatory T Cell Function. J. Exp. Med. *196*, 851–857.
61. Cheng, L.E., Ohlén, C., Nelson, B.H., and Greenberg, P.D. (2002). Enhanced signaling through the IL-2 receptor in CD8+ T cells regulated by antigen recognition results in preferential proliferation and expansion of responding CD8+ T cells rather than promotion of cell death. Proc. Natl. Acad. Sci. USA *99*, 3001–3006.
62. Graßhoff, H., Comdühr, S., Monne, L.R., Müller, A., Lamprecht, P., Riemekasten, G., and Humrich, J.Y. (2021). Low-Dose IL-2 Therapy in Autoimmune and Rheumatic Diseases. Front. Immunol. *12*, 648408.
63. Chinen, T., Kannan, A.K., Levine, A.G., Fan, X., Klein, U., Zheng, Y., Gasteiger, G., Feng, Y., Fontenot, J.D., and Rudensky, A.Y. (2016). An essential role for IL-2 receptor in regulatory T cell function. Nat. Immunol. *17*, 1322–1333.
64. Hosseini, A., Gharibi, T., Marofi, F., Babaloo, Z., and Baradaran, B. (2020). CTLA-4: From mechanism to autoimmune therapy. Int. Immunopharm. *80*, 106221.
65. Chatenoud, L., and Bluestone, J.A. (2007). CD3-specific antibodies: a portal to the treatment of autoimmunity. Nat. Rev. Immunol. *7*, 622–632.
66. Kuhn, C., and Weiner, H.L. (2016). Therapeutic anti-CD3 monoclonal antibodies: from bench to bedside. Immunotherapy *8*, 889–906.
67. Hohlfeld, R., and Wekerle, H. (2005). Drug Insight: using monoclonal antibodies to treat multiple sclerosis. Nat. Clin. Pract. Neurol. *1*, 34–44.
68. Martins, F., Sofiya, L., Sykiotis, G.P., Lamine, F., Maillard, M., Fraga, M., Shabafrouz, K., Ribi, C., Cairoli, A., Guex-Crosier, Y., et al. (2019). Adverse effects of immune-checkpoint inhibitors: epidemiology, management and surveillance. Nat. Rev. Clin. Oncol. *16*, 563–580.
69. Tretter, F., Peters, E.M.J., Sturmberg, J., Bennett, J., Voit, E., Dietrich, J.W., Smith, G., Weckwerth, W., Grossman, Z., Wolkenhauer, O., and Marcum, J.A. (2023). Perspectives of (/memorandum for) systems thinking on COVID-19 pandemic and pathology. J. Eval. Clin. Pract. *29*, 415–429.
70. Gardiner, C.W. (1985). Handbook of Stochastic Methods, *3* (springer Berlin).
71. Virtanen, P., Gommers, R., Oliphant, T.E., Haberland, M., Reddy, T., Cournapeau, D., Burovski, E., Peterson, P., Weckesser, W., Bright, J., et al. (2020). SciPy 1.0: fundamental algorithms for scientific computing in Python. Nat. Methods *17*, 261–272.
72. Zi, Z. (2011). Sensitivity analysis approaches applied to systems biology models. IET Syst. Biol. *5*, 336.
73. Sender, R., and Milo, R. (2021). The distribution of cellular turnover in the human body. Nat. Med. *27*, 45–48.

STAR★METHODS

KEY RESOURCES TABLE

REAGENT or RESOURCE	SOURCE	IDENTIFIER
Deposited data		
Relapse Events - Clinical Data	MSOAC consortium	https://doi.org/10.5281/zenodo.8180103
Lymphocyte count - pregnant women	Clalit Database	https://doi.org/10.5281/zenodo.8180103
Relapse Rate of Pregnant Women with MS	Vukusic et al.[48]	https://doi.org/10.5281/zenodo.8180103
Software and algorithms		
Source code	This paper	https://doi.org/10.5281/zenodo.8180103
Python version 3.9.12	Python Software Foundation	https://www.python.org/
Mathematica version 13.2.1	Wolfram Research, Inc.	https://www.wolfram.com/mathematica

RESOURCE AVAILABILITY

Lead contact

Further information and requests for resources should be directed to and will be fulfilled by the lead contact Uri Alon (uri.alon@weizmann.ac.il).

Materials availability

This study did not generate new unique reagents.

Data and code availability

- Data reported in this paper will be shared by the lead contact upon request.
- The source code used to perform the analysis is available at the GitHub repository as of the date of publication. Github repository: https://github.com/YaelLebel/Excitable_Relapses. DOI is listed in the key resources table.
- The data used to perform the analysis is available at the GitHub repository as of the date of publication. Github repository: https://github.com/YaelLebel/Excitable_Relapses. DOI is listed in the key resources table.
- Any additional information required to reanalyze the data reported in this paper is available from the lead contact upon request.

METHOD DETAILS

Relapse-free probability and relapse hazard curves from MSOAC database

The MSOAC database contains data on 4370 relapse events from 1151 different patients. The relapse events in the database are either entered with the exact start date of the event, or with the date it was recorded into the study. The latter can be later than the actual date of the event, and also depends strongly on the clinical visit frequency. To avoid this, we only used relapse entries that had an exact start date recorded. This amounts to 31 patients with 139 relapses total.

For each patient with exact relapse dates we calculated the time differences between consequent relapses after the first relapse. We then calculated the cumulative probability of relapse-free periods. The relapse-free survivability is defined by $S(t) = 1 - CDF(t)$, which is the probability to have a relapse after time shorter than t. The relapse hazard is defined as the probability per unit time of a relapse given by $H(t) = -\frac{d\ log\ S(t)}{dt}$.

Model equations

The dynamics were modeled using two variables - the auto-reactive T-cells (A) and the regulatory T-cells (R). The dynamics are be described by:

$$\frac{dA}{dt} = l_A - m_A A + \gamma A^2\left(1 - \frac{A}{C}\right) - hAR + \sqrt{2\sigma}\xi(t) \quad \text{(Equation 1)}$$

$$\frac{dR}{dt} = l_R - m_R R + \beta AR \quad \text{(Equation 2)}$$

where ξ is Gaussian white noise with mean 0 and standard deviation σ. The parameters are:

- l_A: Rate of production of auto-reactive cells [cell/time].

- l_R: Rate of production of regulatory cells [cell/time].
- m_A: Natural turnover rate of auto reactive cells [1/time].
- m_R: Natural turnover rate of regulatory cells [1/time].
- γ: Reactivity of auto reactive cells to antigen [cell^{-1} time^{-1}].
- C: Carrying capacity of auto reactive cells [cell].
- h: Rate of inhibition of auto reactive cells by regulatory cells [cell^{-1} time^{-1}].
- β: Reactivity of regulatory cells to antigen [cell^{-1} time^{-1}].
- σ: Noise amplitude [cell^2/time].

We assumed that the main mechanism of immune tolerance is regulatory T cells rather than the natural turnover of the autoreactive effector T cells, which means $m_A \ll hR_0$. This sets a typical timescale for the system $\frac{1}{hR_0}$.

Using dimensional analysis we reduced the model to five dimensionless parameters:

$$\frac{dA}{dt} = 1 + GA^2\left(1 - \frac{A}{C}\right) - AR + \sqrt{2\Sigma}\xi(t) \quad \text{(Equation 3)}$$

$$\frac{dR}{dt} = D(1 - R) + BAR \quad \text{(Equation 4)}$$

where the rescaled auto-reactive T-cells are in units of their baseline levels ($A_0 = \frac{l_A}{hR_0} = \frac{l_A m_R}{hl_R}$), the regulatory T-cells are in units of their baseline levels ($R_0 = \frac{l_R}{m_R}$) and time is in units of $\frac{1}{hR_0}$. We assumed that the turnover time of the regulatory cells to be equal to that of the auto-reactive cells. Other assumptions used were $B \ll 1$ (this is necessary in order to have effective shut down of the flare) as well as dimensionless carrying capacity C much larger than all the other dimensionless parameters (needed for large flares).

Adding a white noise term to Equation 4 does not change the conclusions, and thus for simplicity we added noise only to the effector cells in Equation 3. The dimensionless parameters used for the simulations in the main text are shown in Table S1.

First passage time

In order to calculate the average time between flares, we used the Kramer approach,[70] under the assumption that as long the system is not in a flare, the regulatory T-cells are at steady state (i.e., *R=constant*). This allows us to calculate an effective potential for the effector cell equation

$$\frac{dA}{dt} = -\frac{\partial U}{\partial A} + \sqrt{2\sigma}\xi(t)$$

Since we assume that the steady state of both A and R is much smaller than C, namely $A/C \ll 1$, we have:

$$U(A) = -l_A A + \frac{hR_0}{2}A^2 - \frac{\gamma}{3}A^3$$

The potential $U(A)$ has a minimum at the steady state A_{st} and a maximum at A_{th}, above which the system enters the excitable regime. These points are at the zeros of the derivative $\frac{\partial U}{\partial A}$:

$$\frac{\partial U}{\partial A} = l_A - (m_A + hR_0)A - \gamma A^2 = 0$$

$$A_{st} = \frac{hR_0 - \sqrt{(hR_0)^2 - 4\gamma l_A}}{2\gamma}, A_{th} = \frac{hR_0 + \sqrt{(hR_0)^2 - 4\gamma l_A}}{2\gamma}$$

In order to calculate the mean crossing time, we need to calculate the potential difference between these two values. This results in $\Delta U = \frac{(hR_0)^3}{6\gamma^2} - \frac{hR_0 l_A}{\gamma}$, where we used the approximation $\gamma l_A \ll (hR_0)^2$. Using Kramer's approximation[70] the average time to cross the threshold is:

$$T = 2\pi\sqrt{U''(A_{th})U''(A_{st})}exp\left[\frac{\Delta U}{\sigma}\right] \propto hR_0\ exp\left[\frac{(hR_0)^3}{6\gamma^2\sigma} - \frac{hR_0 l_A}{\gamma}\right]$$

Rationale for noise in the A equation

We considered the effect of adding noise to both the A and R equations. Noise in the A equation is far more impactful on the excitability of the systems than noise in the R equation, because to effectively suppress flares, a condition $\beta \ll h$ or equivalently $B \ll 1$ must be met. This leads to a nearly horizontal vector field near the steady state (as depicted in Figures 2A and 2B). Consequently, fluctuations in the vertical direction (i.e., in the R equation) have a lesser influence on the likelihood of crossing the threshold.

A second consideration involves the ability to solve the dynamics analytically. The differential equations lack a potential $U(A, R)$ that can satisfy both $\frac{\partial U}{\partial A} = -\frac{dA}{dt}$ and $\frac{\partial U}{\partial R} = -\frac{dR}{dt}$. As a result, introducing noise to both equations prevents analytical solutions using a Kramers approach. We therefore opted to introduce noise solely in the A equation.

Relapse Shape and Duration

Once a flare is initiated, the dynamics is dominated mostly by the deterministic part of the model. The flare can be divided into three parts, as is seen in Figure 2C. We now analyze the duration of each of the parts:

(1) Rapid exacerbation: this regime is characterized by a quick rise to the carrying capacity C. The dominant part in the A equation is the quadratic and we assume $A<<C$ for most of the way (omitting this assumption has negligible effect on the result). R remains in its steady state to a good approximation. We integrate the equation for the time evolution of A to find:

$$T_1 = \int_{A_{th}}^{C} \frac{dA}{GA^2} \approx \frac{1}{hR_0}$$

(2) Shutdown of the flare by increase of R. The trajectory in phase space slides along the A nullcline (which means $\frac{dA}{dt} = 0$, can be seen in Figure 2B) until $R_{max} = \frac{GC}{4}$. Along the nullcline, since $A \sim C$, we can approximate:

$$A = C - \frac{R}{G}$$

Inserting this into the time evolution for R and integrating we have:

$$T_2 = \int_{R_{st}}^{R_{max} \approx \frac{I'C}{4H}} \frac{dR}{BR\left(C - \frac{R}{G}\right)} \approx \frac{ln\frac{C}{A_0}}{\beta C}$$

(3) Slow shutdown of the regulatory response, with a refractory period. This regime is characterized by a slow decline along the leftmost declining leg of the A nullcline until returning to the steady state (see Figure 2B). In this part of the nullcline we can approximate:

$$A = \frac{1}{R}$$

Inserting this into the time evolution of R and integrating we find:

$$T_3 = \int_{R_{max}}^{R_{st}} \frac{dR}{D+B-DR} \approx \frac{ln\left(\frac{m_R C}{\beta}\right)}{m_R}$$

For further analysis of the effect of parameters on flare shape, see Figure S1 in the supplementary information.

Pregnancy

Using the expression for the first-passage-time, we obtain an expression for the relapse rate: $r = \frac{1}{hR_0} exp\left[-\frac{(hR_0)^3}{6\gamma^2\sigma} + \frac{hR_0 I_A}{\gamma}\right]$. Using this, we estimate the effect that a small change of production rate $I_A \rightarrow (1+\epsilon)I_A$ has on the relapse rate: $r(\epsilon) = r_{baseline}\, exp[q\epsilon]$, with $r_{baseline} = \frac{1}{hR_0} exp\left[-\frac{(hR_0)^3}{6\gamma^2\sigma} + \frac{hR_0 I_A}{\gamma}\right]$ and $q = \frac{hR_0 I_A}{\gamma}$. The baseline level was taken to be $r_{baseline} = 0.64$ which is the baseline (pre-pregnancy) relapse rate in Ref [48] in agreement with the average relapse rate reported more widely in the literature. These relapse rates are shown in table Relapse Rate of Pregnant Women with MS. In order to estimate α we used lymphocyte counts from pregnant women from the Clalit database, which can be seen in table Lymphocyte count - pregnant women in the deposited data. To compute ϵ, we divided the baseline level by the mean lymphocyte count at each week of pregnancy and postpartum. Since the lymphocyte count is provided by weeks, we averaged over 13 week periods to match the relapse data measured in trimesters. Fitting employed the Levenberg-Marquardt algorithm through Scipy's curve_fit() tool,[71] with a single fit parameter q.

Sensitivity analysis

Sensitivity of variable v to parameter q is defined as.

$Sensitivity(p) = \frac{d\ log\ v}{d\ log\ p}$[72]

We used a first order Taylor expansion to determine the sensitivity of the relapse rate to each of the parameters. The sensitivities are listed in Table S2.

Alternative models

Ratiometric inhibition of A by R

We analyzed a model variant in which inhibition of A by R is described as a ratio with R in the denominator, instead of a difference. The model equations are:

$$\frac{dA}{dt} = l_A - m_A A + \frac{\gamma}{R} A^2 \left(1 - \frac{A}{C}\right)$$

$$\frac{dR}{dt} = l_R - m_R R + \beta A$$

The parameters have the same biological meaning (even though some have different units) as those presented in the model equations part.

Although the nullclines in this model shows the classical N-shape that allows for excitability, the range of parameters needed for excitability did not result in strong spikes with high amplitude of A.

Dynamics limited by self-tissue

We also analyzed a model variant in which the autoimmune attack is limited by the loss of self-tissue target, rather than by the regulatory T-cells denoted R. This model has two variables: autoreactive cells (A) and healthy tissue (H). The model equations are:

$$\frac{dA}{dt} = l_A - m_A A + \beta\gamma H A^2 \left(1 - \frac{A}{C}\right)$$

$$\frac{dH}{dt} = l_H - m_H H - \beta H A$$

With the following parameters: l_H $\left[\frac{cells}{time}\right]$: production rate of healthy tissue cells. m_H $\left[\frac{1}{time}\right]$: natural removal rate of healthy tissue cells. $\frac{1}{m_H}$ is the turnover rate of the healthy tissue. $\frac{l_H}{m_H}$ is the steady state of the healthy tissue without auto-immune killing ($\beta = 0$). β $\left[\frac{1}{cells \cdot time}\right]$: autoimmune killing rate. l_A, m_A are the same as l_H, m_H but for the auto-immune cells. γ $\left[\frac{1}{cells}\right]$: the stimulation rate of A due to self antigen released by killing. C [*cells*] carrying capacity of A.

This model has an intrinsic separation of timescale because the typical turnover of the auto-reactive cells is on the order of hours to days, whereas the typical turnover rate of tissues is of the order of weeks or longer.[73] This separation of timescales allows for analysis similar to the FitzHugh-Nagumo model. In this model, the flare is shut off when the healthy tissue level declines close to zero. This stands in contrast to observations that regulatory T-cells are mainly responsible for the shutdown of the flare. Moreover, in MS and other diseases, the healthy tissue (e.g., myelinating oligodendrocytes in MS) does not seem to decline to zero upon a flare up. Therefore we preferred the model in the main text.